

Microwave processing of magnesium based materials: a review

W. L. E. Wong¹, K. S. Tun², M. Gupta^{2*}

¹*School of Engineering, PSB Academy, 2985 Jalan Bukit Merah Singapore 159457*

²*Department of Mechanical Engineering, National University of Singapore, 9 Engineering Drive 1, Singapore 117576*

Received 29 October 2010, received in revised form 14 March 2011, accepted 15 March 2011

Abstract

Magnesium based materials were synthesized and characterized in this study using an innovative hybrid microwave sintering technique. Different nano-size reinforcements comprising of silicon carbide, alumina, yttria, copper and nickel were used to reinforce pure magnesium. Composites were prepared using blend-compact-microwave sintering-extrusion methodology. Results revealed that properties of magnesium can be convincingly enhanced using the said processing methodology and the material formulations selected. Most importantly, the study established the viability of microwave sintering approach used in place of conventional sintering for magnesium based formulations.

Key words: magnesium, nano-reinforcements, microwave sintering, mechanical properties

1. Introduction

Magnesium is the lightest of all engineering metals with a density of 1.74 g cm^{-3} which is two-thirds the density of aluminum (2.7 g cm^{-3}) and one-fourth that of steel ($\sim 7.8 \text{ g cm}^{-3}$) [1–4] and is comparable with plastics [5]. Densities of plastics can range from 0.90 g cm^{-3} for polypropylene to 2.20 g cm^{-3} for polytetrafluoroethylene [5]. Common reinforcing materials for polymeric composites include glass fibers (2.58 g cm^{-3}) and carbon fibers ($1.78\text{--}2.15 \text{ g cm}^{-3}$) and the resultant reinforced plastics have densities which are comparable with magnesium alloys. Although polymeric materials have comparable density with magnesium, its limited service temperature (generally below 300°C), susceptibility to degradation by UV rays and difficulties in repairing of plastics restrict their applications.

Magnesium exhibits growing demand for its increased usage in recent years due to growing global environmental awareness for improved energy efficiency with the aim of conserving resources and reducing harmful greenhouse gas emissions. In the transport industry, magnesium has been used in vehicular structural frames, engine components, external body panels, etc. to replace steel in an effort to reduce weight and increase fuel economy. In electronic and commu-

nication industries, magnesium casings have been used in electronic devices for the replacement of plastics due to their high strength-to-weight ratio, good electromagnetic shielding properties, excellent heat dissipation and recyclability [1–4]. However, there are still certain limitations such as higher cost, fabrication issues and lower strength than steel and aluminum that prevent magnesium from being used more widely.

In order to enable the wider applications of magnesium metal in the various industries, research efforts are underway to synthesize new and high performance magnesium based materials and to develop more efficient processing techniques. Common methods used to improve the strength of magnesium include alloying and the addition of stiffer and stronger ceramic and/or metallic reinforcements. However, the addition of micron-size reinforcements generally deteriorates the ductility of the matrix [4, 6]. In recent years, studies have revealed that the addition of nano-size reinforcements helped to improve the mechanical properties of magnesium [7, 8]. In addition, the use of a small volume fraction of nano-size reinforcements have been shown to produce results comparable or even superior to that of MMCs reinforced with higher volume fraction of micron size reinforcements [7, 8].

Magnesium has traditionally been processed using liquid casting or powder metallurgy technique.

*Corresponding author: tel.: +65 6516 6358; fax: +65 6779 1459; e-mail address: mpegm@nus.edu.sg

Table 1. Properties of materials used

Material	Purity	Size range	Manufacturer
<i>Matrix</i>			
Magnesium	98.5 %	60–300 μm	Merck KGaA, Germany
<i>Reinforcement</i>			
Copper	99 + %	50 nm	Argonide Corporation, USA
Copper	99.8 %	25 nm	Nanostructured & Amorphous Materials, USA
Nickel	99.9 + %	20 nm	Nanostructured & Amorphous Materials, USA
Silicon carbide	–	45–55 nm	Nanostructured & Amorphous Materials, USA
Alumina	–	50 nm	Baikowski, USA
Yttria	–	30–50 nm	Inframat Advanced Materials, USA

For powder metallurgy, sintering is an important step that serves to instill strength and formation of bonds between particles. Sintering is typically carried out by using electricity to heat resistive elements which in turn transfer the thermal energy to the material via electromagnetic radiation. This process is often the most time-consuming process in the powder metallurgy route.

Microwave heating is an emerging technology that can be used for the rapid and efficient heating of a wide range of different materials [9–12]. Some of the advantages of microwave heating include reduction in processing time, volumetric and uniform heating, selective and controlled heating, improved properties, environmental friendliness and potential in the synthesis and processing of novel and/or nanostructured materials [9–12]. Magnesium based materials synthesized using a hybrid microwave sintering technique was first reported by Gupta and Wong [13]. The results revealed an improvement in hardness and tensile properties of microwave sintered magnesium when compared to conventional sintered magnesium. Further work was carried out by the same group of researchers to investigate the effects of microwave sintering on various types of magnesium based materials.

Accordingly, this review aims to consolidate the work done so far on selected magnesium based materials reinforced with different types of ceramic and/or metallic reinforcements synthesized using hybrid microwave sintering [13–21].

2. Experimental procedures

2.1. Materials

The compositions of materials used in this study are listed in Table 1. Pure magnesium was used as the matrix material. Various types of nano-size reinforcements were used to evaluate their effect in enhancing the performance of magnesium. For MgCu composites, copper nano-particles of 50 nm in size were employed

while in $\text{MgY}_2\text{O}_3\text{Cu}$ hybrid composite, 25 nm copper nano-particles were used.

2.2. Processing

Pure magnesium powder and nano-size reinforcements were weighed carefully and blended in a RETSCH PM-400 mechanical alloying machine using a speed of 200 rpm for 60 min. No balls or process control agent was used during this blending step. The blended powders were uniaxially compacted using a pressure of 97 bar (~ 50 t) to billets (40 mm height with 35 mm diameter) in a 100 t press. The compacted billets were sintered using an innovative microwave assisted hybrid sintering technique for a specific duration to approximately 640°C in a 900 W, 2.45 GHz SHARP microwave oven using SiC as the microwave susceptor material [13, 14]. All magnesium compacts were then sintered under ambient atmospheric condition without the presence of inert gas atmosphere. A schematic diagram of the experimental setup is shown in Fig. 1. Temperature calibration of the sintering setup was performed beforehand using a sheathed K-type thermocouple in order to determine the appropriate sintering duration for the billets. In the present study, the heating rate for the setup can be varied by changing the amount of SiC susceptor used. The higher heating rate ($49^\circ\text{C min}^{-1}$) was realized by using maximum possible amount of susceptor (400 g) that was possible in the present experimental setup. The lower heating rate ($20^\circ\text{C min}^{-1}$) was realized using a smaller amount of susceptor (300 g) [19]. Pure magnesium was compacted using the same pressure as the composite formulations and sintered in microwave oven under identical conditions. For benchmarking purposes, conventional sintering was carried out using a Carbolite tube furnace in an argon controlled environment. A heating rate of $10^\circ\text{C min}^{-1}$ was used to heat pure magnesium metal compact to a sintering temperature of 0.85 of the melting temperature for pure magnesium, which corresponds to 785 K (512°C), and held at this temperature for 120 min before cool-

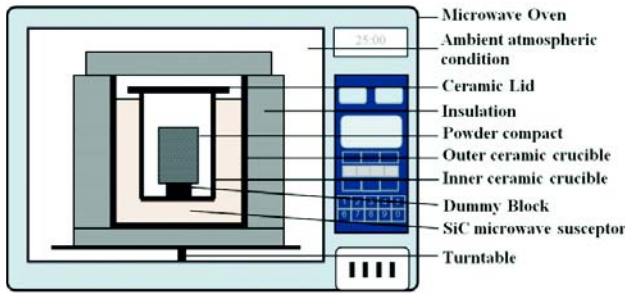


Fig. 1. Schematic diagram of experimental setup used in this study.

ing. The cooling rate was a constant $25\text{ }^{\circ}\text{C min}^{-1}$. The sintered billets of pure magnesium and its composite formulations were subsequently hot extruded at a temperature of $350\text{ }^{\circ}\text{C}$ using an extrusion ratio of 25 : 1 on a 150 t hydraulic press using colloidal graphite as lubricant to produce an extruded rod with a final diameter of 7 mm. In a study on extrusion ratio, two additional extrusion ratios of 12 : 1 and 19 : 1 were used [18].

2.3. Density measurements

The densities of the extruded samples were determined using Archimedes principle. Polished samples taken from various sections of the extruded rods were weighed in air and then immersed in distilled water using an A&D electronic balance with an accuracy of $\pm 0.0001\text{ g}$. Theoretical densities of the sample were calculated based on the rule-of-mixtures principle.

2.4. Microstructure characterization

Microstructural characterization studies were conducted on polished specimens of pure Mg and its composite formulations to investigate the presence of porosity and reinforcement distribution. The samples were examined using a scanning electron microscope (SEM) and a field emission scanning electron microscope (FE-SEM).

2.5. X-ray diffraction

X-ray diffraction analysis was carried out on the polished samples of extruded monolithic Mg and Mg composites using an automated Shimadzu XRD-6000 diffractometer. The samples were exposed to $\text{Cu K}\alpha$ radiation ($\lambda = 1.54056\text{ \AA}$) at a scanning speed of 2 deg min^{-1} . The Bragg angle, θ , and the values of the interplanar spacing d obtained were subsequently matched with the standard values for Mg and other related phases.

2.6. Mechanical properties characterization

Macrohardness testing was performed on the as-sintered compacts prior to extrusion to determine the hardness distribution across the compacts. Macrohardness was measured on the Rockwell 15T Superficial Scale using a 1.588 mm (1/16 inch) steel ball indenter with test load of 15 kgf and dwell time of 2 s. The hardness measurements were performed using a Future-Tech FR-3 Rockwell Type Hardness Tester in accordance with ASTM standard E18-02.

Microhardness measurements were performed on the polished samples of extruded magnesium based materials using a Matsuzawa MXT 50 automatic digital microhardness tester. The microhardness test was performed using a Vickers indenter under a test load of 25 gf and a dwell time of 15 s in accordance with the ASTM standard E384-99.

Tensile properties of the extruded Mg and its composites samples were determined in accordance with ASTM standard E8M-01. The tensile tests were conducted on round tension test specimens of 5 mm in diameter and 25 mm gauge length using an automated servohydraulic testing machine (MTS 810) with a crosshead speed set at 0.254 mm min^{-1} .

2.7. Fracture behavior

Fracture surface characterization studies were performed on the pure Mg and composite specimens tested under tension in order to provide an insight into the various possible fracture mechanisms operative during the tensile loading of the samples. Fractography was accomplished utilizing a JEOL JSM-5600LV SEM.

3. Results and discussion

3.1. Hybrid microwave heating

Microwave heating of materials is fundamentally different from conventional heating due to the way heat transfer takes place in the material. In a conventional furnace, thermal energy is usually transferred to the material via thermal electromagnetic radiation in the infrared region from the external heating elements. Due to the limited penetration depth of infrared radiation ($D_p \ll 10^{-4}\text{ m}$) in most solids [22], energy deposition is restricted to the surface of the material and heat transfer to the rest of the material is based on thermal conduction. Therefore during conventional heating, the temperature at the core of the material is usually lower than the temperature at the surface. The penetrative power of microwaves allows heat to be generated from within the material itself as a result of the absorption of microwave energy by the

Table 2. Analysis of energy consumption between conventional and microwave sintering during heating

Material	Heating unit	Power (kW)	Time (h/min)	Energy consumption (kWh)	Energy savings (%)
Magnesium	Tube furnace (Carbolite CTF15/75)	6	0.82/49	4.92	–
	Microwave (Sharp magnetron)	1.6*	0.22/13	0.35	93
		1.6*	0.42/25	0.67	86
		1.6*	0.53/32	0.85	83

* Based on AC power required for operation of the magnetron

material directly and does not depend on the thermal conduction of heat from the surfaces. Since heat is generated from within the volume of the material and radiates outwards, the temperature at the center is usually higher than the temperature at the surface.

To minimize the temperature variation in the material, a hybrid heating method is adopted in this study using microwaves and SiC powder. SiC powder (contained within a microwave transparent ceramic crucible) absorbs microwave energy readily at room temperature and is heated up quickly, providing the radiant heat to heat the billet externally while the compacted billet absorbs microwaves and is heated from within. This hybrid heating method results in a more uniform temperature gradient within the billet and circumvents the disadvantage of heating using either conventional heating or microwaves only. Materials produced by this method have been shown to demonstrate better properties than materials synthesized using conventional sintering [12, 13].

3.2. Advantages of hybrid microwave heating

The main advantages of microwave sintering are shorter processing time and significant energy efficiency over conventional sintering. For conventional sintering of pure magnesium, the total sintering time required is 169 min (based on a heating rate of $10^{\circ}\text{C min}^{-1}$ from room temperature to 512°C with no intermittent isothermal holding time and a 2 h soaking duration at 512°C). Microwave sintering was performed by heating the compacts to a temperature of approximately 640°C for a duration of 13, 25 and 32 min depending on the amount of SiC susceptor used without any holding time. Assuming the cooling rate to be almost identical for both conventional and microwave sintering, this translates to a reduction of 81 % to 92 % in processing time.

A comparison of the energy consumption during sintering of magnesium using a conventional tube furnace and a microwave oven is shown in Table 2. Comparing the heating cycle (not including the holding time for conventional sintering) for both processes, it can be observed that the use of microwave sintering can lead to an impressive energy savings of more than

83 % without detrimental effects on the end properties of magnesium which is economically viable for industries and environmentally friendly in the reduction of CO_2 emissions.

During conventional sintering, the heating rate is limited by two factors; firstly, the capability of the furnace to achieve fast heating rates (due to slow resistive heating of the heating elements) and secondly, to prevent large thermal variation within the compacts to avoid cracking or warpage. The slower heating rate, the need for holding at intermittent temperature to reduce thermal variation and long soaking time for sintering increases the total processing time of the compacts. For microwave heating coupled with external susceptors, rapid heating rates in excess of $20^{\circ}\text{C min}^{-1}$ can be easily achieved since the powder compact can absorb microwave energy directly and be heated rapidly from within. External susceptors provide radiant heating to the samples externally thereby reducing the thermal variation in the compacts. This is supported by macrohardness measurements conducted on the as-sintered compacts which revealed a lesser degree of variation in hardness across the diameter of the compact for microwave sintered magnesium compared to conventionally sintered magnesium. The macrohardness distribution across conventionally and microwave sintered compacts are reproduced in Fig. 2.

In addition to a significant reduction in processing time, the current methodology using microwaves and SiC susceptors also demonstrated the viability of sintering highly reactive magnesium metal at high temperature without the need for an inert protective atmosphere unlike in conventional sintering. Most importantly, the end properties of microwave sintered magnesium (which will be discussed in later sections) are not affected by the absence of an inert atmosphere during sintering. This can lead to considerable cost savings and can be further investigated for applicability to other metallic systems.

3.3. Selection of reinforcements

Three different types of nano-size reinforcements were selected for addition into magnesium matrix. Firstly, silicon carbide was selected because it is an

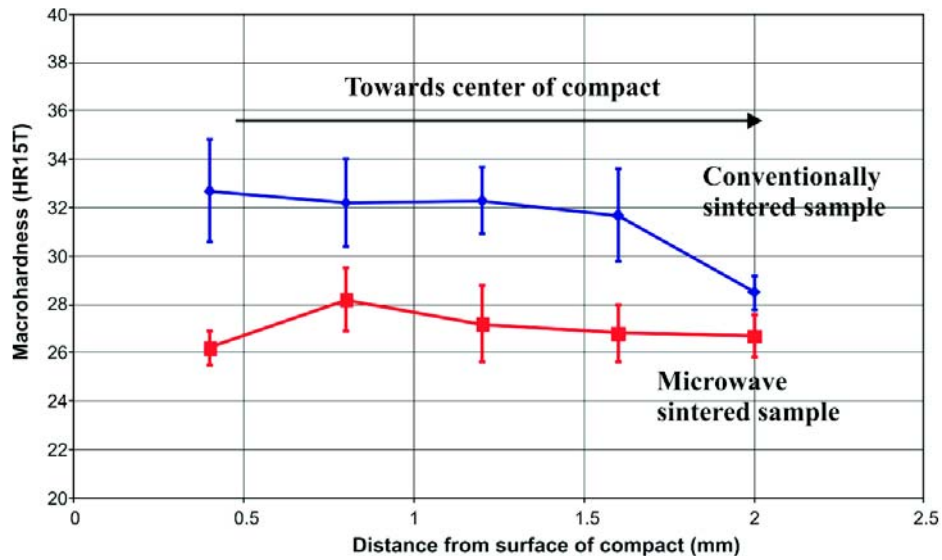


Fig. 2. Macrohardness distribution across conventionally and microwave sintered compacts.

Table 3. Results of density and porosity measurements

Materials	Reinforcement		Theoretical ρ	Experimental ρ	Porosity
	(vol.%)	(wt.%)	(g cm ⁻³)	(g cm ⁻³)	(%)
Mg Conv	–	–	1.740	1.737 ± 0.002	0.15
Mg MW (32 min)	–	–	1.740	1.734 ± 0.002	0.33
Mg MW (25 min)	–	–	1.740	1.737 ± 0.001	0.17
Mg MW (13 min)	–	–	1.740	1.738 ± 0.007	0.13
Mg composites					
Mg0.35SiC	0.35	0.65	1.745	1.735 ± 0.003	0.58
Mg0.5SiC	0.5	0.92	1.747	1.739 ± 0.002	0.48
Mg1.0SiC	1.0	1.84	1.755	1.753 ± 0.007	0.11
Mg0.3Al ₂ O ₃	0.3	0.7	1.747	1.741 ± 0.004	0.32
Mg0.6Al ₂ O ₃	0.6	1.4	1.753	1.742 ± 0.008	0.67
Mg1.0Al ₂ O ₃	1.0	2.25	1.762	1.756 ± 0.001	0.83
Mg/0.3Cu	0.3	1.5	1.762	1.758 ± 0.002	0.19
Mg/0.6Cu	0.6	3.0	1.783	1.776 ± 0.006	0.41
Mg1.0Cu	1.0	4.91	1.812	1.809 ± 0.007	0.13
Mg0.17Y ₂ O ₃	0.17	0.5	1.746	1.73 ± 0.01	0.87
Mg0.7Y ₂ O ₃	0.7	2.0	1.763	1.757 ± 0.006	0.35
Hybrid composites					
Mg0.7Y ₂ O ₃ 0.3Ni	0.7	0.3 ^a	1.785	1.778 ± 0.002	0.34
Mg0.7Y ₂ O ₃ 0.6Ni	0.7	0.6 ^a	1.806	1.802 ± 0.002	0.21
Mg0.7Y ₂ O ₃ 1.0Ni	0.7	1.0 ^a	1.835	1.829 ± 0.002	0.30
Mg0.7Y ₂ O ₃ 0.3Cu	0.7	0.3 ^a	1.784	1.775 ± 0.001	0.45
Mg0.7Y ₂ O ₃ 0.6Cu	0.7	0.6 ^a	1.806	1.792 ± 0.004	0.77

^a Represents volume fraction of 2nd reinforcement

excellent microwave susceptor and can be rapidly heated from room temperature when exposed to microwaves at a frequency of 2.45 GHz. Secondly, alumina and yttria were selected because they are microwave transparent and cannot be heated easily at room temperature using microwaves at a frequency of

2.45 GHz due to its low dielectric loss. Lastly, metallic copper and nickel powders which are electrical conducting materials were selected. It has been shown by other investigators that metallic powders can be heated up rapidly using 2.45 GHz microwaves [23, 24].

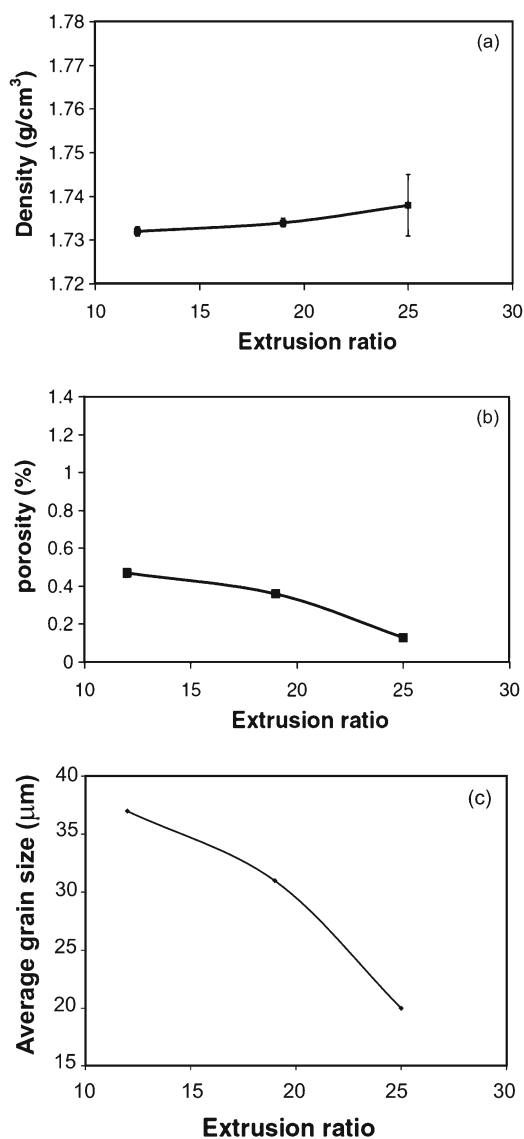


Fig. 3. Effect of extrusion ratio on the (a) density, (b) porosity and (c) grain size of pure magnesium.

3.4. Macrostructure

The results of macrostructural characterization on the sintered billets revealed absence of sintering defects such as circumferential or radial cracks even though the heating rates are as high as $49^{\circ}\text{C min}^{-1}$. Following extrusion, no observable macro defects were observed on monolithic Mg and Mg composite samples. The outer surface was smooth and free of circumferential cracks.

3.5. Density and porosity

Near theoretical density can be realized for microwave sintered magnesium and composite formulations after extrusion. For pure magnesium, the density

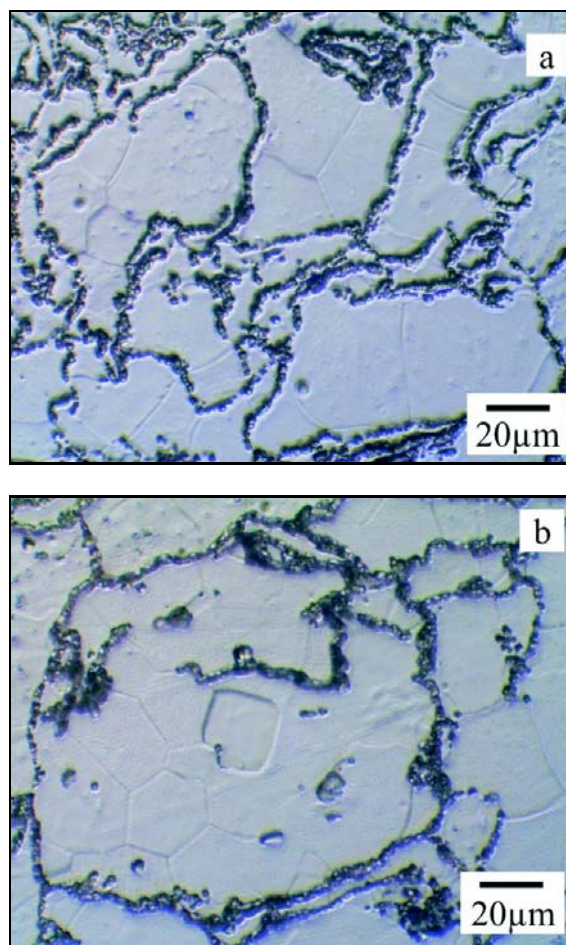


Fig. 4. Representative optical micrographs showing the etched microstructure of: (a) conventionally sintered Mg and (b) hybrid microwave sintered Mg.

and porosity of microwave sintered magnesium that were sintered at faster heating rates (or shorter time duration of 13 and 25 min) are comparable with conventional sintered magnesium in spite of the significant reduction in process time. The results of porosity measurements amongst the microwave sintered magnesium indicate that higher heating rate leads to an improvement in the densification of magnesium (Table 3).

When varying the extrusion ratio of the compacts after hybrid microwave sintering, it was observed that there is an increase in density (corresponding decrease in porosity) with an increase in extrusion ratio. This is due to the higher compressive forces generated with increasing extrusion ratio and is in agreement with previous studies that reported a reduction in porosity with increasing extrusion ratio [6, 25]. Data from the study [18] are reproduced in Fig. 3. Further work is on-going to determine the optimum processing parameters to achieve better densification.

Composite formulations also displayed low poros-

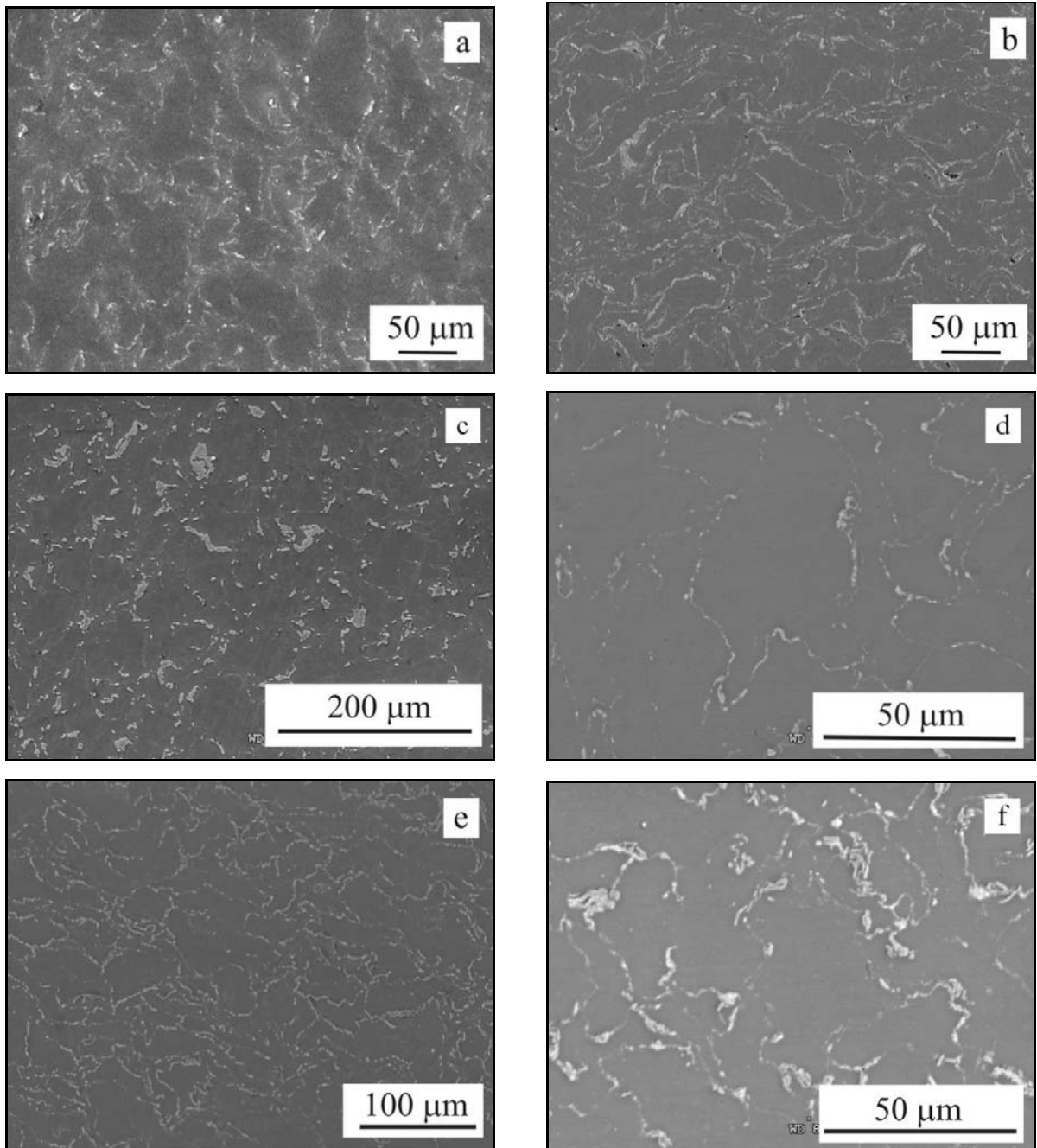


Fig. 5. Representative micrographs showing the distribution of reinforcements in: (a) Mg_{0.5}SiC, (b) Mg_{1.0}Al₂O₃, (c) Mg_{1.0}Cu, (d) Mg_{0.7}Y₂O₃, (e) Mg_{0.7}Y₂O₃0.3Cu and (f) Mg_{0.7}Y₂O₃0.6Ni.

ity values with the highest porosities exhibited by MgAl₂O₃ and MgY₂O₃ formulations. As shown in Table 3, MgAl₂O₃ displayed increasing porosity values with increasing volume fraction of Al₂O₃. The higher porosities shown by MgAl₂O₃ and MgY₂O₃ formulations may be caused by the poor coupling of 2.45 GHz microwaves with these ceramic particles. MgSiC formulations displayed decreasing porosity values with increasing volume fraction of SiC with Mg_{1.0}SiC achieving the lowest porosity value of 0.11 %. This may be attributed to SiC being an

excellent microwave susceptor. Magnesium reinforced with copper nanopowder exhibited moderate porosity value that was in close comparison with SiC. This may be attributed to the ability of copper powders to heat in both the electric and magnetic fields [24] and also due to the formation of liquid Mg₂Cu phase [15] which aid in densification during sintering. Hybrid composites also displayed low porosity values with the maximum porosity of 0.77 % exhibited by Mg_{0.7}Y₂O₃0.6Cu. No significant trend in porosity values was observed with in-

creasing volume fraction of metallic reinforcement added.

3.6. Microstructural characterization

Microstructural characterization studies revealed minimal porosity in the samples congruent with the results of density measurements. Finer microstructure can be observed in microwave sintered pure magnesium when compared to its conventionally sintered counterpart as shown in Fig. 4. Magnesium compact sintered at faster heating rate also displayed smaller average grain size of $20 \pm 3 \mu\text{m}$ than its counterpart sintered at lower heating rate with an average grain size of $36 \pm 9 \mu\text{m}$ [19]. This can be attributed to the shorter processing time for microwave sintering which leads to minimal microstructure coarsening. Similarly, the average grain size decreases with increasing extrusion ratio for pure magnesium as shown in Fig. 3c.

Microstructure characterization conducted on microwave sintered and extruded composite samples revealed the presence of a network of nano-sized particulates decorating the particle boundaries of the matrix (Figs. 5a–f) similar to that observed by other researchers working on aluminum and magnesium based composites reinforced with nanoparticles [26–28]. Similar fabrication technique involving blending of powders, compaction, sintering and extrusion were employed in these studies, the main difference lies in the method of sintering (conventional resistance heating versus microwave heating). The micrographs revealed the presence of minimal porosity which is also supported by the results of experimental density measurements (Table 3). Figure 6 shows a micrograph of etched Mg1.0Cu sample, where Cu particles and intermetallic phases (denoted by bright regions) are located primarily along the grain boundaries. Result of EDX analysis confirmed the presence of Mg and Cu phases. For hybrid composites, micrographs also showed the presence of metallic particles, intermetallics and yttria which are confirmed by EDX analysis as shown in Fig. 7.

3.7. X-ray diffraction

X-ray diffraction studies conducted on Mg and its composite formulations were able to detect the presence of pure Mg and Ni peaks and Mg_2Cu and Mg_2Ni intermetallic peaks. For Mg reinforced with SiC, Al_2O_3 and Y_2O_3 nanoparticles, only Mg phase was detected, while the SiC, Al_2O_3 and Y_2O_3 phases were not detected at all. This can be attributed to the limitation of the filtered X-ray to detect phases with less than 2 vol.% [29]. For Mg reinforced with 1 vol.% of Cu nanoparticles, Mg_2Cu reaction phase was detected. The formation of Mg_2Cu phase was due to reaction between Cu and Mg phases when sintered

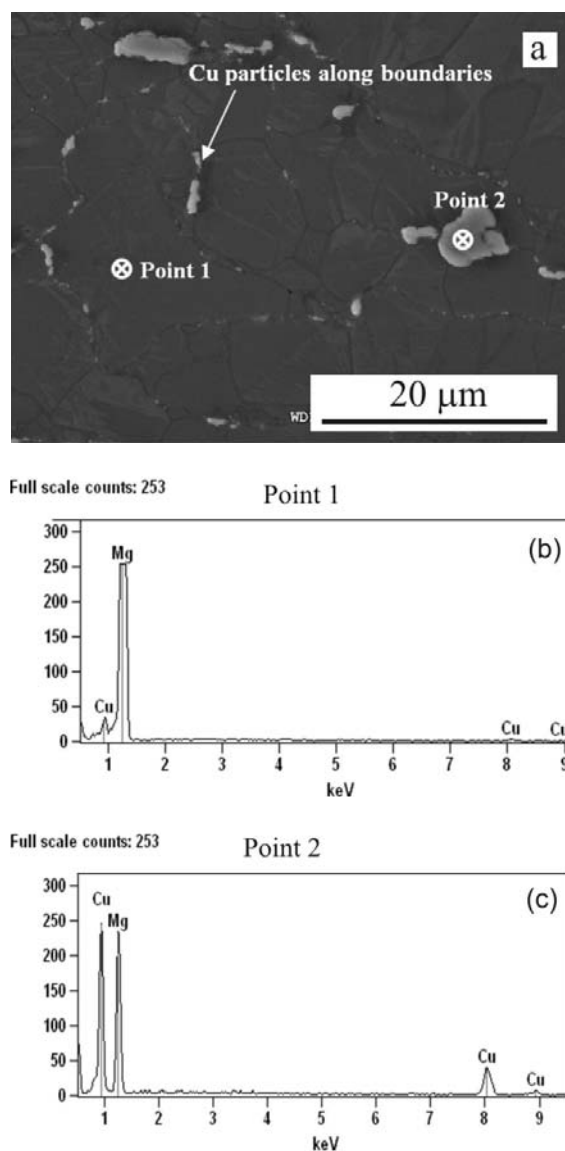
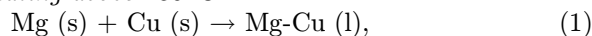


Fig. 6. Micrograph showing the distribution of Cu particles and phases along grain boundaries in etched Mg1.0Cu sample and EDX analysis showing the presence of Mg and Cu phases.

above the eutectic temperature of 485°C according to the following equations [29, 30]:

Heating above 485°C :



Cooling below 485°C :



where (s) denotes the solid state and (l) the liquid state.

Similarly in $\text{MgY}_2\text{O}_3\text{Ni}$ hybrid composites, the formation of Mg_2Ni phase was due to reaction between Ni and Mg phases when sintered above the eutectic temperature of 506°C [30]. XRD patterns for MgCu

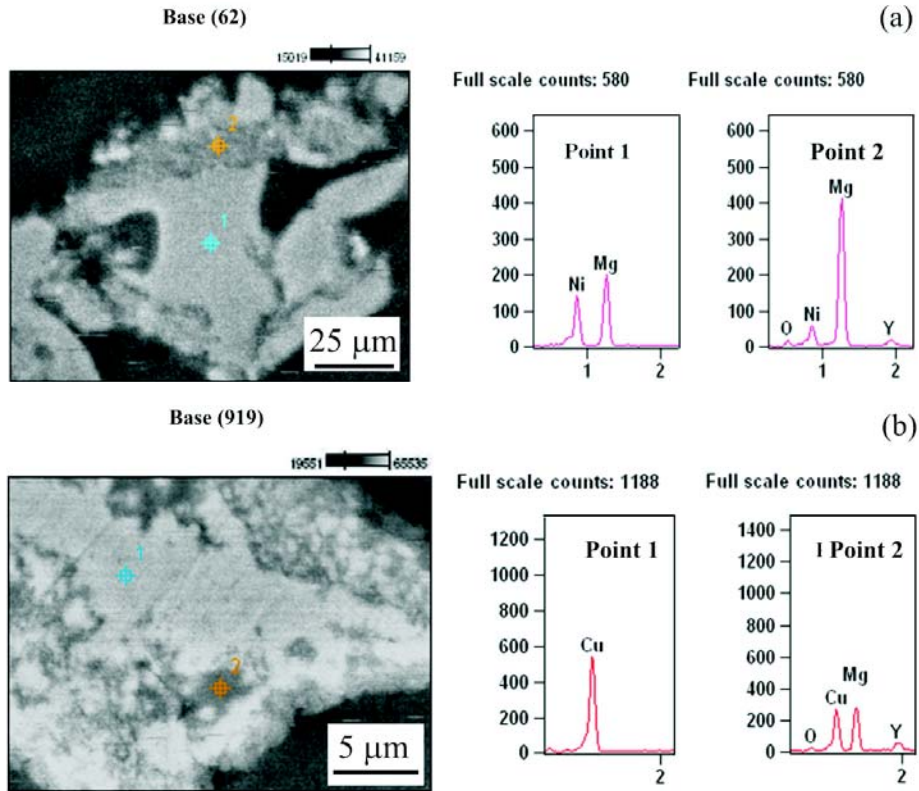


Fig. 7. Micrographs and EDX analysis showing the presence of (a) nickel, yttria and Mg_2Ni intermetallic in Mg matrix for $Mg_{0.7}Y_2O_3_{0.6}Ni$ and (b) copper, yttria and Mg_2Cu intermetallic in Mg matrix for $Mg_{0.7}Y_2O_3_{0.6}Cu$.

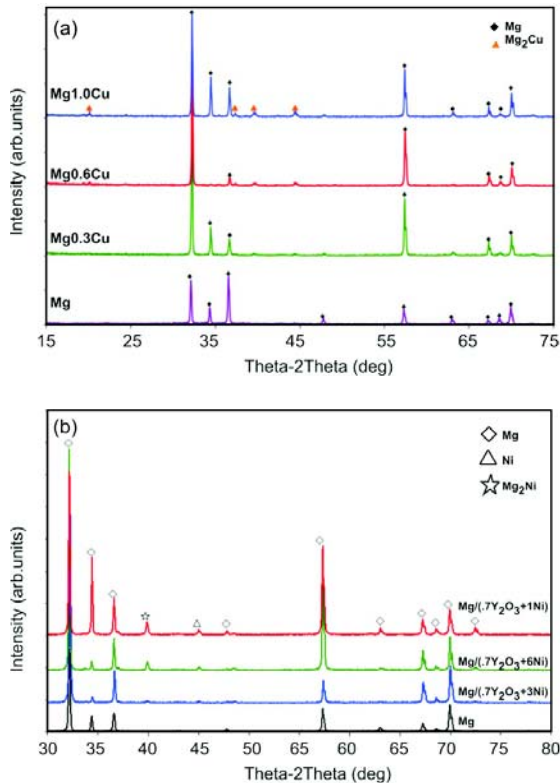


Fig. 8. X-ray diffractograms of $MgCu$ and MgY_2O_3Ni composites.

composites and MgY_2O_3Ni hybrid composites are reproduced in Fig. 8.

3.8. Mechanical characterization

Microhardness of microwave sintered magnesium is comparable with conventionally sintered magnesium. For Mg MW (25 min), the microhardness was observed to be marginally higher when compared to conventionally sintered magnesium. This finding is consistent with the results of other investigators where it has been shown that microwave sintered metal compacts have higher hardness than their conventionally sintered counterparts [11, 31]. The increase in hardness (Table 4) of magnesium matrix with the addition of nano-size reinforcements can be attributed primarily to: (i) presence of harder nanopowder reinforcements in the matrix and (ii) higher constraint to the localized matrix deformation due to the presence of harder phases.

The results of tensile testing revealed an improvement in 0.2%YS and UTS for all the composite formulations investigated (Table 4). The largest improvement in strength was shown by $Mg_{0.6}Cu$ composite formulation with an improvement of ~ 96 % in 0.2%YS, ~ 54 % in UTS and no change in failure strain over pure Mg sintered for 25 min. The increase in 0.2%YS and UTS can be attributed to: (i) work

Table 4. Mechanical properties of monolithic Mg and Mg nanocomposites

Materials	Microhardness HV	0.2%YS (MPa)	UTS (MPa)	Failure strain (%)
Mg conv	37 ± 1	105 ± 0	150 ± 1	5.0 ± 0.7
Mg MW (32 min)	36 ± 2	116 ± 17	186 ± 21	11.3 ± 1.0
Mg MW (25 min)	40 ± 1	121 ± 2	176 ± 2	5.4 ± 0.7
Mg MW (13 min)	37 ± 2	134 ± 7	193 ± 1	6.9 ± 2.5
Mg composites				
Mg0.35SiC	40 ± 1	132 ± 14	194 ± 11	6.3 ± 1.0
Mg0.5SiC	42 ± 1	144 ± 12	194 ± 10	7.0 ± 2.0
Mg1.0SiC	43 ± 2	157 ± 22	203 ± 22	7.6 ± 1.5
Mg0.3Al ₂ O ₃	48 ± 3	119 ± 7	175 ± 8	7.5 ± 0.2
Mg0.6Al ₂ O ₃	54 ± 3	130 ± 5	180 ± 7	7.4 ± 0.3
Mg1.0Al ₂ O ₃	60 ± 4	155 ± 3	216 ± 13	5.7 ± 0.5
Mg/0.3Cu	49 ± 1	188 ± 13	218 ± 11	5.9 ± 1.1
Mg/0.6Cu	52 ± 2	237 ± 24	286 ± 8	5.4 ± 1.2
Mg1.0Cu	60 ± 3	194 ± 11	221 ± 17	2.9 ± 0.4
Mg0.17Y ₂ O ₃	38 ± 0	144 ± 2	214 ± 4	8.0 ± 2.8
Mg0.7Y ₂ O ₃	45 ± 2	157 ± 10	244 ± 1	8.6 ± 1.2
Hybrid composites				
Mg0.7Y ₂ O ₃ 0.3Ni	54 ± 4	221 ± 7	262 ± 6	9.0 ± 0.9
Mg0.7Y ₂ O ₃ 0.6Ni	60 ± 4	232 ± 8	272 ± 2	9.5 ± 0.9
Mg0.7Y ₂ O ₃ 1.0Ni	63 ± 4	228 ± 8	271 ± 6	5.5 ± 0.7
Mg0.7Y ₂ O ₃ 0.3Cu	–	215 ± 20	270 ± 22	11.1 ± 1.0
Mg0.7Y ₂ O ₃ 0.6Cu	–	179 ± 7	231 ± 13	11.1 ± 0.7

Table 5. Comparison of improvement in mechanical properties over matrix material

Materials	Improvement in mechanical properties over matrix material (%)		
	0.2%YS	UTS	Failure strain
Mg MW (25 min)		Reference material	
Mg1.0SiC	30	15	41
Mg1.0Al ₂ O ₃	28	23	6
Mg0.6Cu	96	63	0
Mg MW (13 min)		Reference material	
Mg0.7Y ₂ O ₃	17	26	25
Mg0.7Y ₂ O ₃ 0.6Ni	73	41	38
Mg0.7Y ₂ O ₃ 0.3Cu	60	40	61
<i>Micrometer-scale reinforcement</i>			
Mg/12.8SiC ¹	2	–12	–88
ZC63/12SiC ²	7	–19	–92
AZ91/10SiC ³	–20	–29	–59
Mg/2.1Cu ⁴	181	30	–67
<i>Nanometer-scale reinforcement</i>			
Mg/1.11 Al ₂ O ₃ ⁵	47	30	64
Mg/3.0SiC ⁶	–20	–4	–54

¹ Data from [36] (DMD + extrusion)² Data from [37] (Casting, T6 treated)³ Data from [38] (PM + extrusion)⁴ Data from [39] (DMD + extrusion)⁵ Data from [28] (PM + extrusion)⁶ Data from [26] inferred from tensile graph (PM + extrusion)

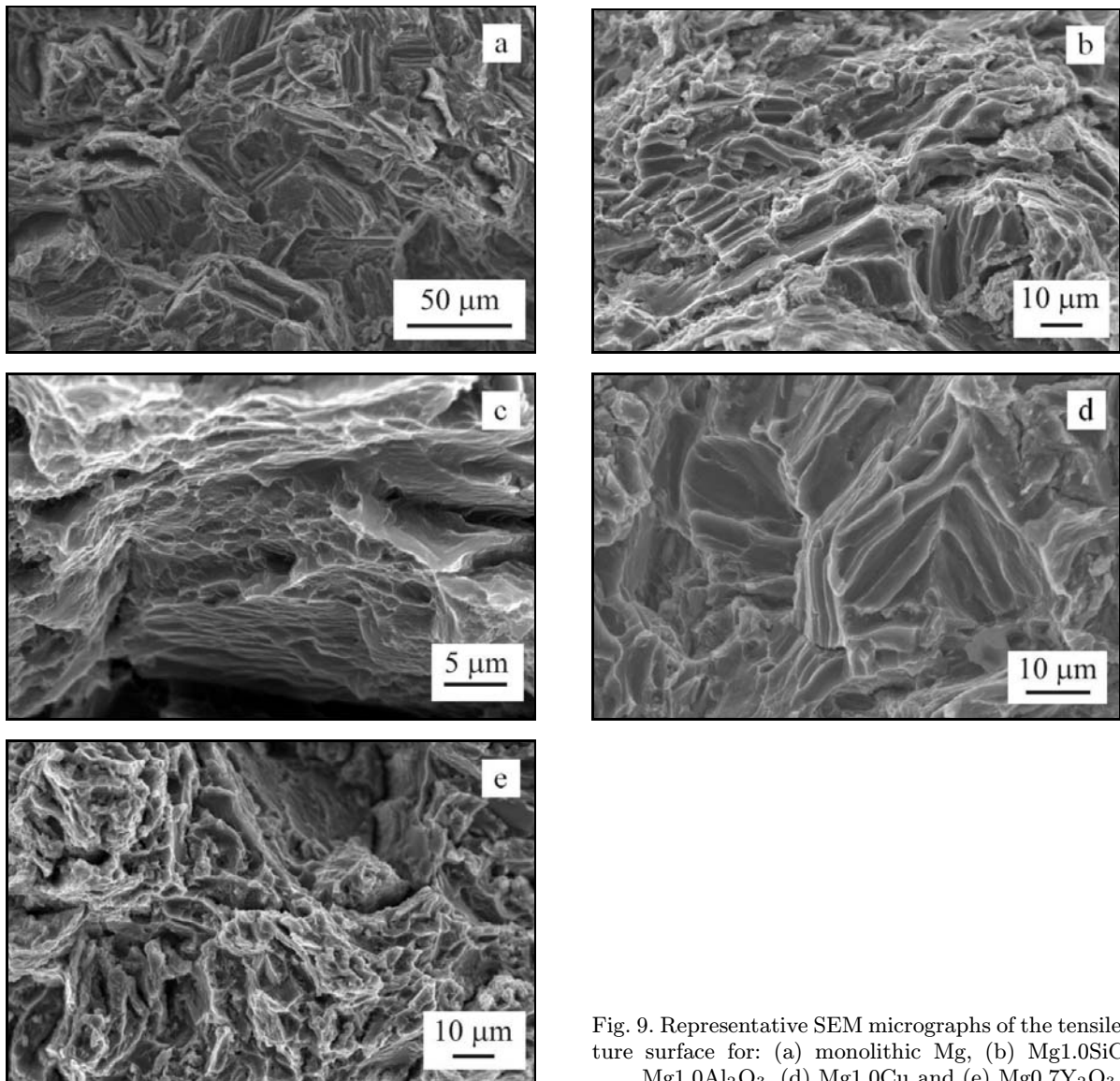


Fig. 9. Representative SEM micrographs of the tensile fracture surface for: (a) monolithic Mg, (b) Mg1.0SiC, (c) Mg1.0Al₂O₃, (d) Mg1.0Cu and (e) Mg0.7Y₂O₃.

hardening due to the strain misfit between the reinforcing particulates and the matrix, (ii) the formation of internal thermal stresses due to different thermal expansion behavior between the nano reinforcements and the matrix, (iii) Orowan strengthening [4, 6], (iv) reduction in grain size and (v) effective load transfer between matrix and reinforcements.

Increase in failure strain with the addition of nano-size SiC, Al₂O₃ and Y₂O₃ may be attributed to the activation of non-basal slip [32]. Increase in ductility has also been observed in the past when Ti [33], Mo [34], CNT [35] and nano-Al₂O₃ [28] was added to Mg. The reduction in failure strain for MgCu composites can be attributed to the coupled presence of harder copper reinforcement and brittle Mg₂Cu intermetallic phase in the matrix which lead to plastic incompatibility and serve as potential crack initiation sites. Similar trend was also observed in MgY₂O₃Ni hybrid composites

with the addition of 1.0 vol.% of nickel reinforcement.

A comparison of the improvement in mechanical properties of Mg nanocomposites synthesized in this study with other Mg composites strengthened with micrometer-scale reinforcement [36–39] and nanometer-scale reinforcement [26, 28] are shown in Table 5. Mg MW (25 min) was used as the reference material for comparison with magnesium composites reinforced with SiC, Al₂O₃ and Cu while Mg MW (13 min) was used as the reference material for the MgY₂O₃ and hybrid composites. It can be seen that in general, the addition of nanometer-scale SiC, Al₂O₃ and Y₂O₃ ceramic reinforcements can lead to a simultaneous improvement in strength and failure strain of the matrix material (except in the last case where Mg is reinforced with 3 vol.% of nanometer-scale SiC). The magnitude of improvement in 0.2%YS is also typically higher for nano-size reinforcements with the ex-

ception of Mg reinforced with micrometer-scale copper. Comparing Mg reinforced with 1 and 3 vol.% of nanometer-scale SiC (2nd row and last row in Table 5), it can be seen that the mechanical properties in addition to being dependent on the volume fraction of reinforcements added, are also dependent on the processing methodology. Sintering using both microwaves and radiant heat (hybrid sintering) can produce improvement in both strength and failure strain.

3.9. Fracture behavior

The results of fracture surface analysis revealed a predominantly brittle fracture in the case of Mg samples (Fig. 9a). This can be attributed to the HCP crystal structure of magnesium that restricts the plastic deformation to $\{0001\} \langle 11\bar{2}0 \rangle$ basal slip and $\{10\bar{1}2\} \langle 10\bar{1}1 \rangle$ pyramidal twinning at temperature below 498 K [3]. The presence of cleavage steps and microscopically rough fracture surface indicates the inability of magnesium to deform significantly under uniaxial tensile loading. For the Mg composite formulations, the fracture surface revealed a predominantly brittle fracture with refined fracture features (Figs. 9b–e).

4. Conclusions

1. It has been shown convincingly that the properties of magnesium can be enhanced using a combination of microwaves and radiant heat from external susceptors for sintering.

2. Microstructural characterization revealed finer microstructure for microwave sintered magnesium when compared to conventionally sintered magnesium.

3. The nanometer-scale reinforcements formed a continuous network along the grain boundaries of the matrix.

4. Mechanical characterization revealed an increase in hardness, 0.2%YS and UTS of magnesium with the addition of nanometer-scale reinforcements. Failure strain was improved with the addition of SiC, Al₂O₃ and Y₂O₃ ceramic reinforcements but displayed the opposite trend with the addition of higher volume fraction of metallic reinforcement.

5. The use of microwave sintering in place of conventional sintering can lead to a significant reduction in processing time without compromising the end properties of the material. Additionally, it also allows the sintering of reactive magnesium metal without the aid of a protective inert atmosphere.

Acknowledgements

Authors wish to acknowledge the Agency for Science,

Technology and Research Grant 092 137 0015 (WBS# R-265-000-321-305) for supporting this work.

References

- [1] MORDIKE, B. L.—KAINER, K. U. (Eds.): Magnesium alloys and their applications. Frankfurt, Germany, Werkstoff-Informationsgesellschaft 1998.
- [2] MORDIKE, B. L.—EBERT, T.: Mater. Sci. Eng. A, 302, 2001, p. 37. doi:10.1016/S0921-5093(00)01351-4
- [3] NEITE, G.—KUBOTA, K.—HIGASHI, K.—HEHMANN, F.: In: Materials Science and Technology. Vol. 8. Eds.: Cahn, R. W., Haasen, P., Kramer, E. J. Germany, Wiley-VCH 2005, p. 115.
- [4] MOLL, F.—KAINER, K. U.: In: Magnesium Alloys and Technology. Ed.: Kainer, K. U. Weinheim, Wiley-VCH 2002, p. 197.
- [5] CALLISTER, W. D.: Materials Science and Engineering: An Introduction. 7th Ed. New York, John Wiley & Sons Inc. 2006.
- [6] LLOYD, D. J.: Int. Mater. Rev., 39, 1994, p. 1.
- [7] HASSAN, S. F.—GUPTA, M.: J. Mater. Sci., 41, 2006, p. 2229. doi:10.1007/s10853-006-7178-3
- [8] GOH, C. S.—WEI, J.—LEE, L. C.—GUPTA, M.: Mater. Sci. Eng. A, 423, 2006, p. 153. doi:10.1016/j.msea.2005.10.071
- [9] STEIN, D. F. (Chairman): Microwave Processing of Materials. National Materials Advisory Board. Washington, D.C., National Academy Press 1994.
- [10] CLARK, D. E.—SUTTON, W. H.: Annu. Rev. Mater. Sci., 26, 1996, p. 299. doi:10.1146/annurev.ms.26.080196.001503
- [11] ROY, R.—AGRAWAL, D.—CHENG, J.—GEDEVANISHVILI, S.: Nature, 399, 1999, p. 668. doi:10.1038/21390
- [12] GUPTA, M.—WONG, W. L. E.: Microwaves and Metals. Singapore, John Wiley & Sons (Asia) Pte Ltd. 2007.
- [13] GUPTA, M.—WONG, W. L. E.: Scripta Mater., 52, 2005, p. 479. doi:10.1016/j.scriptamat.2004.11.006
- [14] WONG, W. L. E.—GUPTA, M.: Adv. Eng. Mater., 8, 2006, p. 735. doi:10.1002/adem.200500209
- [15] WONG, W. L. E.—GUPTA, M.: Compos. Sci. Technol., 67, 2007, p. 1541. doi:10.1016/j.compscitech.2006.07.015
- [16] WONG, W. L. E.—GUPTA, M.: Adv. Eng. Mater., 9, 2007, p. 902. doi:10.1002/adem.200700169
- [17] TUN, K. S.—GUPTA, M.: Compos. Sci. Technol., 67, 2007, p. 2657. doi:10.1016/j.compscitech.2007.03.006
- [18] TUN, K. S.—GUPTA, M.: J. Mater. Sci., 43, 2008, p. 4503. doi:10.1007/s10853-008-2649-3
- [19] TUN, K. S.—GUPTA, M.: J. Alloys and Compounds, 466, 2008, p. 140. doi:10.1016/j.jallcom.2007.11.047
- [20] TUN, K. S.—GUPTA, M.: J. Alloys and Compounds, 487, 2009, p. 76. doi:10.1016/j.jallcom.2009.07.117
- [21] TUN, K. S.—GUPTA, M.—SRIVATSAN, T. S.: Mater. Sci. Tech., 26, 2010, p. 87. doi:10.1179/174328408X388095
- [22] BYKOV, Y. V.—RYBAKOV, K. I.—SEMENOV, V. E.: J. Phys. D: Appl. Phys., 34, 2001, p. 55. doi:10.1088/0022-3727/34/13/201
- [23] WALKIEWICZ, J. W.—KAZONICH, G.—MCGILL, S. L.: Miner. Metall. Proc., 5, 1988, p. 39.

- [24] CHENG, J.—ROY, R.—AGRAWAL, D.: Mater. Res. Innov., 5, 2002, p. 170. [doi:10.1007/s10019-002-8642-6](https://doi.org/10.1007/s10019-002-8642-6)
- [25] KAWAMURA, Y.—KATO, H.—INOUE, A.—MASUMOTO, T.: Mater. Sci. Eng. A, 219, 1996, p. 39. [doi:10.1016/S0921-5093\(96\)10437-8](https://doi.org/10.1016/S0921-5093(96)10437-8)
- [26] FERKEL, H.—MORDIKE, B. L.: Mat. Sci. Eng. A, 298, 2001, p. 193. [doi:10.1016/S0921-5093\(00\)01283-1](https://doi.org/10.1016/S0921-5093(00)01283-1)
- [27] KANG, Y. C.—CHAN, S. L.: Materials Chemistry and Physics, 85, 2004, p. 438. [doi:10.1016/j.matchemphys.2004.02.002](https://doi.org/10.1016/j.matchemphys.2004.02.002)
- [28] HASSAN, S. F.—GUPTA, M.: Mat. Sci. Eng. A, 392, 2005, p. 163. [doi:10.1016/j.msea.2004.09.047](https://doi.org/10.1016/j.msea.2004.09.047)
- [29] CULLITY, B. D.: Elements of X-ray Diffraction. 3rd ed. London, Prentice Hall 2001.
- [30] OKANOTO, H. (ed.): Desk Handbook: Phase Diagrams for Binary Alloys. Ohio Park, ASM International 1993.
- [31] ANKLEKAR, R. M.—BAUER, K.—AGRAWAL, D. K.—ROY, R.: Powder Metall., 48, 2005, p. 39. [doi:10.1179/003258905X37657](https://doi.org/10.1179/003258905X37657)
- [32] AGNEW, S. R.—DUYGULU, O.: Int. J. Plasticity, 21, 2005, p. 1161. [doi:10.1016/j.ijplas.2004.05.018](https://doi.org/10.1016/j.ijplas.2004.05.018)
- [33] HASSAN, S. F.—GUPTA, M.: J. Alloy Compd., 345, 2002, p. 246. [doi:10.1016/S0925-8388\(02\)00413-9](https://doi.org/10.1016/S0925-8388(02)00413-9)
- [34] WONG, W. L. E.—GUPTA, M.: Adv. Eng. Mater., 7, 2005, p. 250. [doi:10.1002/adem.200400137](https://doi.org/10.1002/adem.200400137)
- [35] GOH, C. S.—GUPTA, M.—WEI, J.—LEE, L. C.—LIM, K. W.: Development of magnesium nanocomposites with carbon nanotubes reinforcements. Presented at Thin Films and Nanotech 2004, Singapore 2004.
- [36] GUPTA, M.—LAI, M. O.—SARAVANARANGANTHAN, D.: J. Mater. Sci., 35, 2000, p. 2155. [doi:10.1023/A:1004706321731](https://doi.org/10.1023/A:1004706321731)
- [37] HOLDEN, P. E.—PILKINGTON, R.—LORIMER, G. W.—KING, J. F.—WILKS, T. E.: In: Proceedings of 3rd International Magnesium Conference. London, The Institute of Materials 1997, p. 647.
- [38] CHUA, B. W.—LU, L.—LAI, M. O.: Composite Structures, 47, 1999, p. 595. [doi:10.1016/S0263-8223\(00\)00031-3](https://doi.org/10.1016/S0263-8223(00)00031-3)
- [39] HASSAN, S. F.—GUPTA, M.: Mater. Sci. Technol., 19, 2003, p. 253. [doi:10.1179/026708303225009346](https://doi.org/10.1179/026708303225009346)